*Accelerated Publication*

THE JOURNAL OF BIOLOGICAL CHEMISTRY
Vol. 277, No. 28, Issue of July 12, pp. 24851–24854, 2002
*Printed in U.S.A.*

# The Crystal Structure of the Endothelial Protein C Receptor and a Bound Phospholipid*

Received for publication, March 20, 2002,
and in revised form, May 23, 2002
Published, JBC Papers in Press, May 28, 2002,
DOI 10.1074/jbc.C200163200

**Vaheh Oganesyan‡, Natalia Oganesyan§, Simon Terzyan¶, Dongfeng Qu‡, Zbigniew Dauter‖, Naomi L. Esmon**, and Charles T. Esmon‡§**‡‡§§**

*From the ‡Cardiovascular Biology Research Program, §Howard Hughes Medical Institute, and ¶Department of Crystallography, Oklahoma Medical Research Foundation, Oklahoma City, Oklahoma 73104, ‖SAIC/NCI-Frederick, National Institutes of Health, Frederick, Maryland 21702, and the Departments of **Pathology and ‡‡Biochemistry and Molecular Biology, University of Oklahoma Health Sciences Center, Oklahoma City, Oklahoma 73104*

**The endothelial cell protein C receptor (EPCR) shares ~20% sequence identity with the major histocompatibility complex class 1/CD1 family of molecules, accelerates the thrombin-thrombomodulin-dependent generation of activated protein C, a natural anticoagulant, binds to activated neutrophils, and can undergo translocation from the plasma membrane to the nucleus. Blocking protein C/activated protein C binding to the receptor inhibits not only protein C activation but the ability of the host to respond appropriately to bacterial challenge, exacerbating both the coagulant and inflammatory responses. To understand how EPCR accomplishes these multiple tasks, we solved the crystal structure of EPCR alone and in complex with the phospholipid binding domain of protein C. The structures were strikingly similar to CD1d. A tightly bound phospholipid resides in the groove typically involved in antigen presentation. The protein C binding site is outside this conserved groove and is distal from the membrane-spanning domain. Extraction of the lipid resulted in loss of protein C binding, which could be restored by lipid reconstitution. CD1d augments the immune response by presenting glycolipid antigens. The EPCR structure is a model for how CD1d binds lipids and further suggests additional potential functions for EPCR in immune regulation, possibly including the anti-phospholipid syndrome.**

For blood to clot, a series of sequential proteolytic complexes form, each leading to the generation of a new serine protease (1). The complexes contain the zymogen, a membrane-bound enzyme, a cofactor protein, and $Ca^{2+}$ ions all assembled on a negatively charged phospholipid surface. Complete complex assembly is essential to rapid activation of the bound zymogen. In most cases, binding of the zymogen and the protease to the membrane is mediated by a specialized vitamin K-dependent domain containing γ-carboxyglutamic acid (Gla, and referred to as the Gla domain). For these complexes to function efficiently, it is critical that negatively charged phospholipids be mobilized to the cell surface, an event that requires a potent cell agonist (2).

Balancing the clotting system are several natural anticoagulant mechanisms. One of the most potent is the protein C anticoagulant pathway. The critical nature of the pathway is demonstrated by the clinical observation that homozygous deficiency results in neonatal or embryonic lethality in man and mice (for review, see Ref. 3). Protein C activation occurs on the surface of the endothelium when thrombin binds to thrombomodulin (for review, see Ref. 4). Activated protein C (APC)[1] generated by this complex then binds to protein S on negatively charged membrane surfaces and inactivates the critical cofactors, factors Va and VIIIa, preventing further thrombin generation.

Recently protein C activation has been shown to be augmented by EPCR. Direct binding of protein C to EPCR circumvents the requirement for endothelial cell activation for these cells to support protein C activation effectively (5). Binding of protein C to EPCR has been shown to be mediated almost entirely by the vitamin K-dependent Gla domain (6), normally considered to be primarily involved in binding to negatively charged phospholipid surfaces.

In addition to binding protein C, EPCR appears to perform other functions. It binds proteinase 3, the autoantigen in Wegener's granulomatosis. This complex then binds to Mac-1 on activated neutrophils (7) where it apparently inhibits tight leukocyte adhesion to activated endothelium. The proteinase 3 and protein C binding sites appear to be distinct. Another property of EPCR is that it can translocate from the membrane surface to the nucleus.

EPCR shares sequence homology with the major histocompatibility complex class 1 (MHC class 1) and CD1 family of molecules (8). In general, these molecules bind ligands in a deep hydrophobic groove formed by two α-helices that overlie the eight-stranded β-pleated sheet (9). CD1 molecules can bind lipid antigens and present these antigens to T cells. Like the CD1 molecules, the structure presented here indicates that EPCR has its groove filled with a lipid molecule, but unlike the CD1 molecules, EPCR is missing the α3 domain and does not associate with $\beta_2$-microglobulin. Mutagenesis studies of EPCR have indicated that protein C binding is mediated at the tip of EPCR and does not involve the groove (10).

## EXPERIMENTAL PROCEDURES

*Recombinant Soluble EPCR (rsEPCR) Purification, Crystallization, and Structure Determination*—rsEPCR was expressed and purified es-

* This research was supported by Specialized Centers of Research Grant P50 HL54502 awarded by the National Institutes of Health. The costs of publication of this article were defrayed in part by the payment of page charges. This article must therefore be hereby marked "*advertisement*" in accordance with 18 U.S.C. Section 1734 solely to indicate this fact.

*The atomic coordinates and structure factors (code 1L8J and 1LQV) have been deposited in the Protein Data Bank, Research Collaboratory for Structural Bioinformatics, Rutgers University, New Brunswick, NJ (http://www.rcsb.org/).*

§§ An Investigator for the Howard Hughes Medical Institute. To whom correspondence should be addressed: Howard Hughes Medical Inst., Oklahoma Medical Research Foundation, 825 N. E. 13th St., Oklahoma City, OK 73104. Tel.: 405-271-7571; Fax: 405-271-3137; E-mail: Charles-Esmon@omrf.ouhsc.edu.

[1] The abbreviations used are: APC, activated protein C; EPCR, endothelial cell protein C receptor; MHC, major histocompatibility complex; rsEPCR, recombinant soluble EPCR; HUVEC, human umbilical vein endothelial cell; FL-APC, fluorescently labeled APC.

TABLE I
*Data collection, phasing, and refinement statistics*

PC, protein C; pCMB, *p*-chloromercuribenzoate.

| Data set | Native | $K_2Pt(SCN)_6$ | pCMB | rsEPCR-PC Gla domain |
|---|---|---|---|---|
| Wavelength (Å) | 0.97 | 1.54 | 1.54 | 1.54 |
| Resolution (Å) | 20–2.0 | 50–2.6 | 50–2.8 | 50–1.55 |
| Completeness (%) | 99.6 (96.1) | 97.9 (98.8) | 99.5 (99.1) | 98.0 (83.8) |
| Multiplicity/overall $I/\sigma$ | 5/40 | 10/25 | 8/6.5 | 10/34 |
| $R_{merge}$[a] | 3.8 (25.7) | 6.5 (35.0) | 7.5 (34.5) | 5.0 (45.5) |
| Phasing statistics | | | | |
| *R*-factor (%) | | 16.5 | 22.3 | |
| Phasing power | | 1.55 | 1.38 | |
| $R_{cullis}$[b] | | 0.68 | 0.72 | |
| Figure of merit | 0.82 | | | |
| Refinement statistics | | | | |
| $R_{cryst}/R_{free}$[c] (%) | 19.5/22.0 | | | 18.9/20.5 |
| Number of atoms | 1618 | | | 4032 |

[a] $R_{merge} = \Sigma|I - \langle I\rangle|/\Sigma I$.
[b] $R_{cullis} = \Sigma||F_{ph} - \langle F_p\rangle| - |F_h||/\Sigma|F_{ph} - \langle F_p\rangle|$.
[c] $R_{cryst} = \Sigma|F_{obs} - F_{calc}|/\Sigma F_{obs}$; $R_{free}$ calculated as $R_{cryst}$ but on 5% of data aside of refinement.

sentially as described previously (11) except that the Chinese hamster ovary cell line Lec 3.2.8.1 was used for expression to shorten the *N*-linked carbohydrates. rsEPCR was concentrated to 15 mg/ml in TBS (20 mM Tris-HCl, pH 7.5, 100 mM NaCl), 0.02% $NaN_3$. 4 M sodium formate was used as a precipitant. Crystals were grown in hanging drops by the vapor diffusion method. Data collection for the native form was performed with a synchrotron x-ray source (National Synchrotron Light Source, X9B) where the crystal diffracted to 2.0 Å and for derivatives was performed on a MAR345 image plate detector (MAR Research, Norderstedt, Hamburg, Germany) mounted on a Rigaku rotating anode x-ray generator (MSC, The Woodlands, TX) and equipped with an Oxford cooling system. The crystals of human rsEPCR belong to the $P3_121$ space group with the cell parameters a = b = 69.6 Å, c = 96.0 Å. The asymmetric unit contains one rsEPCR molecule. The data were processed using the HKL2000 package (12). The rsEPCR crystal in 6 M sodium formate, TBS, and 0.02% $NaN_3$ was soaked overnight at room temperature with $10^{-4}$ M $K_2Pt(SCN)_6$. Three binding sites were revealed. When the rsEPCR crystal in 4 M sodium formate, TBS, and 0.02% $NaN_3$ was soaked overnight in $10^{-4}$ M *p*-chloromercuribenzoate, three derivatized sites were also detected. After solvent flattening and density modification, the phases were used to calculate the electron density map. The electron density was clearly interpretable and allowed placement of 150 consecutive residues. All the calculations were done using CNS (13). Model building was performed using O software (14). Data statistics and procedure results are summarized in Table I.

*rsEPCR-Protein C Crystallization and Structure Determination*—Protein C was isolated from a vitamin K-dependent protein concentrate (a generous gift from Baxter AG) essentially as described previously (15). rsEPCR was mixed with protein C at a ratio of 1.1 to 1. The mixture in TBS, 10 mM $CaCl_2$, and 0.02% $NaN_3$ was concentrated to 20 mg/ml. The crystallization condition was: 100 mM KCl, 10 mM $MgCl_2$, 10 mM $CaCl_2$, 50 mM HEPES, pH 7.0, and 5% (v/v) polyethylene glycol. The crystal was washed for 5–10 s in 100 mM KCl, 10 mM $MgCl_2$, 10 mM $CaCl_2$, 50 mM HEPES, pH 7.0, and 22% (v/v) polyethylene glycol 400 and then flash cooled on the goniometer head. The resolution limit of the diffraction was about 1.55 Å on the in-house machine. Data were processed using HKL2000. Data statistics are summarized in Table I. The crystal belongs to the $P2_1$ space group with cell parameters a = 59.22 Å, b = 62.36 Å, c = 71.03 Å, $\beta$ = 101.81°. The asymmetric unit contains two complexes.

*EPCR-APC Binding Assay*—Briefly, rsEPCR was used as a competitor to block the binding of active site fluorescently labeled APC to human umbilical vein endothelial cells (HUVECs) (11, 16). Inhibition of APC binding was analyzed by flow cytometry (16).

*Extraction of Phospholipid from rsEPCR*—All extraction experiments were performed at room temperature. 1 ml of 2 mg/ml rsEPCR in TBS, 5 mM EDTA was mixed with 100 $\mu$l of 10% Triton X-100. After 1 h, 2 ml of 1-butanol/diisopropyl ether (DIPE) (40:60, v/v) was added, and the sample was rocked overnight at room temperature. The mixture was then centrifuged at 2,000 rpm for 2 min (17). The aqueous phase was removed and washed with pure DIPE to remove possible traces of 1-butanol. The organic phase was evaporated under nitrogen to minimize the possible oxidation of the lipid. The dried organic phase served as the source of lipid for functional reconstitution.

*Reconstitution of rsEPCR-APC Binding Activity*—The delipidated rsEPCR in the aqueous phase was divided into two 300-$\mu$l aliquots. An equal volume of TBS containing 2% *n*-octyl-$\beta$-D-glucopyranoside was added to each aliquot of rsEPCR. No additions were made to the first aliquot of delipidated rsEPCR. To the second aliquot we added 4 $\mu$l of dried lipid extracted from EPCR, and the solution was mixed. The "dried" lipid was a very viscous material that could be pipetted. Tubes were rocked for 2 h at room temperature and then dialyzed overnight against TBS.

## RESULTS AND DISCUSSION

To help elucidate how EPCR carries out its wide range of functions, we solved the structure of rsEPCR alone and also bound to the Gla domain of protein C. Although the crystal packing environments for the two crystals were very different, there appeared to be little change in the EPCR structure upon binding the protein C Gla domain. Specifically the root mean square disposition between two non-crystallographically related rsEPCR molecules in the presence of the protein C Gla domain was as large as the difference seen between either rsEPCR in that structure or the rsEPCR crystal formed in the absence of the protein C Gla domain (root mean square disposition, 0.4 Å). The only large shift involved the side chain of the $Arg^{156}$, which moved to open a hydrophobic pocket in EPCR that can accommodate $Phe^4$ of the protein C Gla domain. The overall fold of rsEPCR is similar to the rest of the members of the MHC class 1 and CD1 families (Fig. 1). A groove is formed by two $\alpha$-helices overlying a $\beta$-pleated sheet. In MHC class 1 molecules that bind peptides, the distance between the $\alpha$-helices is larger than in rsEPCR or CD1d. Although the CD1d x-ray structure has been solved (18), the lipid molecule was not modeled. The rsEPCR and the CD1d molecules were superimposed to compare the lipid binding grooves. The comparison revealed that of 18 residues making contacts between rsEPCR and the lipid molecule, seven are identical, and six residues have similar properties in CD1d (Fig. 2). The other five residues are different, but they belong to part of the structure that does not superimpose.

The protein C Gla domain-rsEPCR crystal provided higher resolution data (1.55 Å) than the crystal of rsEPCR (2.0 Å) alone. This higher resolution data allowed us to identify the bound lipid as either phosphatidylethanolamine or phosphatidylcholine (Fig. 1). The fatty acid side chains of the lipid interact with the hydrophobic residues within the groove. The helices cover these fatty acid side chains, apparently restricting solvent access (Fig. 3) and perhaps protecting the fatty acids from oxidation. The head group is solvent-exposed compromising exact crystallographic determination.

Although crystallization was attempted between rsEPCR

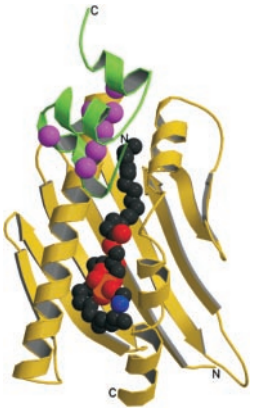


FIG. 1. **The rsEPCR molecule with a portion of the protein C Gla domain and a lipid molecule.** In EPCR (*yellow ribbon*), two $\alpha$-helices and an eight-stranded $\beta$-sheet create a groove that is filled with phospholipid (the space-filling *balls* in the *center*). Binding of $Ca^{2+}$ ions (*magenta spheres*) to the protein C Gla domain (*green ribbon*) exposes the N-terminal $\omega$ loop, which in the absence of EPCR interacts with the phospholipid surfaces on the membrane. There do not appear to be direct interactions between the protein C Gla domain and the lipid molecule located in the groove of rsEPCR. The model of the complex consists of residues 7–177 of rsEPCR and the first 33 residues of the protein C Gla domain (25, 26).

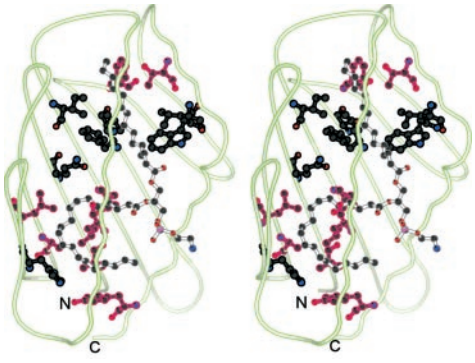


FIG. 2. **Stereodiagram showing the EPCR molecule in coil presentation.** The lipid molecule, and the residues within 3.5Å of the lipid, are represented in the *ball-and-stick* presentation. Superimposition of EPCR and CD1d1 molecules revealed seven identical (shown in *black outline*) and six similar amino acids (shown in *red outline*) within the hydrophobic groove that occupy similar positions. Most of the identical residues are clustered around the *less curved* fatty acid chain, whereas most of the similar ones are around the *kinked* chain. Such clustering might be an indication of the different specificity of EPCR and CD1d1 toward fatty acid chains. Prepared using Molscript (26).

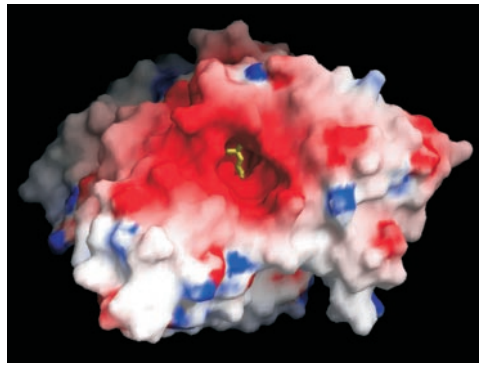

FIG. 3. **Surface representation of the rsEPCR molecule.** Electrostatic potentials are mapped on the surface. The head group of the lipid is solvent-exposed (*yellow stick model* in the *center*), whereas the fatty acid chains are buried deep in the hydrophobic groove (and therefore unseen) (27).

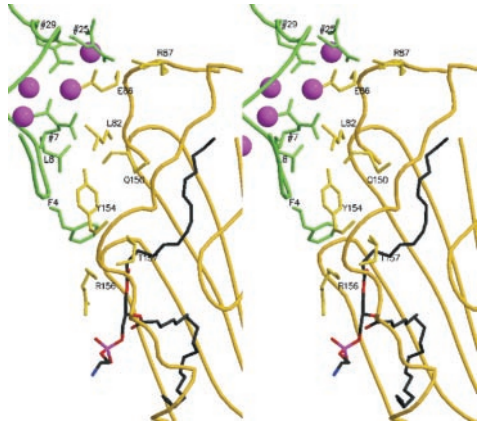


FIG. 4. **The amino acids participating in the interactions between the Gla domain of protein C and rsEPCR.** The *yellow portion* is the interacting region of rsEPCR, the *green portion* is the interacting region of the protein C Gla domain, and the *magenta balls* represent the bound $Ca^{2+}$ ions. The lipid molecule is shown in *black* (25, 26).

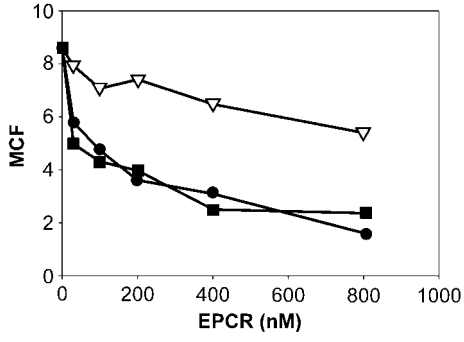


FIG. 5. **The effect of lipid on inhibition of FL-APC binding to HUVECs by the rsEPCR.** FL-APC (60 nM) was mixed with increasing concentrations of wild-type rsEPCR (*circle*), delipidated rsEPCR (*upside down triangle*), and lipid-reconstituted rsEPCR (*square*). The mixtures were added to HUVECs to assay FL-APC binding. All data shown are mean channel fluorescence (*MCF*) *versus* added inhibitor concentration.

and intact protein C, electron density from only the first 33 amino acid residues of protein C could be identified. Positions 42 and 44 in protein C are known to be highly susceptible to cleavage by chymotrypsin-like enzymes. Cleavage at these sites apparently occurred during crystallization. This fortuitous cleavage may have allowed the crystals to form. Binding of protein C to EPCR is $Ca^{2+}$-dependent. The $Ca^{2+}$ ions in the protein C Gla domain (shown in *magenta* in Fig. 1) are clearly visible in the structure. Only one contact is made between the $Ca^{2+}$ ions bound to the protein C Gla domain and EPCR (residue $Glu^{86}$ of EPCR) (Fig. 4). In addition to coordinating one of the $Ca^{2+}$ ions, $Glu^{86}$ is within hydrogen bonding distances from $Gla^{7}$, $Gla^{25}$, and $Gla^{29}$. Other hydrogen bonds between EPCR (first residue) and protein C (second residue) include $Gln^{150}$ to $Gla^{7}$, $Arg^{87}$ to $Gla^{25}$, and $Tyr^{154}$ to $Gla^{7}$. A network of hydrophobic interactions involve $Leu^{82}$-$Gla^{7}$, $Tyr^{154}$-$Phe^{4}$, $Thr^{157}$-$Phe^{4}$, and $Leu^{82}$-$Leu^{8}$. The role of calcium is most likely to help stabilize the hydrophobic "$\omega$" loop of protein C where residues $Phe^{4}$ and $Leu^{8}$ within this loop contribute the majority of the interactions with EPCR. In addition, the $Ca^{2+}$ ions bound to protein C may help to position the Gla residues to facilitate hydrogen bonding interactions with EPCR. The direct contribution of the lipid in EPCR to protein C binding seems to be relatively minor. The closest contact is 4.3 Å away from $Phe^{4}$ of the protein C molecule. However, the fatty acid forms the base of a hydrophobic pocket into which $Phe^{4}$ is inserted. Interestingly $Phe^{4}$ and $Leu^{8}$ of the $\omega$ loop in the protein C appear to be required for protein C binding to phospholipid, which is also a

$Ca^{2+}$ ion-dependent process (19). The $Ca^{2+}$ ions within the Gla domain are in positions very similar to those seen in prothrombin fragment 1 (Protein Data Bank code 2PF2) and factor VIIa (Protein Data Bank code 1DAN).

To determine whether the presence of lipid in the groove is important for protein C binding, the lipid from rsEPCR was extracted and reconstituted with the endogenous lipid extract. Each form was tested for its ability to bind APC measured indirectly by the ability of the rsEPCR to inhibit fluorescently labeled APC binding to endothelial cells that express full-length EPCR (11). Our initial studies indicated that the lipid molecule in rsEPCR was very tightly bound since extensive washing in buffer with or without Triton X-100 failed to remove the bound lipid. Compared with native rsEPCR, lipid extraction reduced the ability of EPCR to block activated protein C binding to HUVECs (Fig. 5). The remaining inhibitory activity could be due either to residual bound lipid or partial retention of activated protein C binding activity. Reconstitution of the lipid derived from rsEPCR restored the inhibitory activity. The lipids alone treated by the reconstitution approach had no inhibitory activity (data not shown). The results suggest that the bound lipid is important for rsEPCR-protein C interaction, possibly related to maintaining EPCR structure.

Some potentially important biological proposals can be derived from the structure. A model of intact APC can be built by annealing the Gla domain shown in this structure with the remainder of the APC structure (20) essentially as described previously (10). The C-terminal tail of EPCR would be inserted into the membrane, while activated protein C would bind at nearly the opposite end of EPCR and point away from the membrane surface. This would be predicted to elevate the active site about 35 $\pm$ 5 Å further from the membrane than would occur if activated protein C were bound directly to phospholipid. The altered distance of the active site from the membrane surface could favor cleavage of cell surface proteins and might contribute to the observed EPCR dependence of some cell signaling events (21).

The structure of EPCR helps to explain why it can function without $\beta_2$-microglobulin and the $\alpha$3 domain. In CD1 proteins, the $\alpha$3 domain is positioned on the opposite side of the $\beta$-sheet from the ligand binding groove and diagonally opposite to the protein C binding site. The residues in the $\beta$-sheet that interact with the $\alpha$3 domain in CD1d are not conserved in EPCR. Hydrophobic interactions exist between the CD1d $\beta$-sheet and $\beta_2$-microglobulin, which is located between $\alpha$1$\alpha$2 and $\alpha$3 domains. Although EPCR has hydrophobic residues at that region, carbohydrates in that region of EPCR would prevent interaction with $\beta_2$-microglobulin.

Despite its relatively small size, EPCR can bind three ligands simultaneously: proteinase 3, protein C/APC, and phospholipid. The lipid is required for protein C binding, but further characterization of the lipid binding specificity of EPCR and analysis of the role of the lipid in cellular trafficking and EPCR-proteinase 3 interactions remain to be completed.

The structure of rsEPCR with its tightly bound phospholipid may provide insights into how CD1 family members bind lipids. Most of the residues contacting the lipid in EPCR are identical or highly conserved in CD1d, suggesting that CD1d binds lipids for antigen presentation in a manner analogous to EPCR. It is tempting to speculate that EPCR may share with CD1d (22) the ability to present lipid antigens, to play a role in host defense from infection, and perhaps, when compromised, to augment autoimmunity. The latter possibility would be consistent with the observation that anti-phospholipid antibodies associated with thrombosis often have a more dramatic impact on the protein C anticoagulant pathway than on procoagulant complexes (23). Given that EPCR-null mice exhibit early embryonic lethality (24), proof of these hypotheses will require improved strategies to acquire viable mice for this analysis.

*Acknowledgments*—We thank T. Burnett and B. Carpenter for help in protein purification; S. N. Barnard for help in manuscript preparation; and O. Safa, K. Hensley, and X. C. Zhang for helpful discussions.

REFERENCES

1. Mann, K. G., Nesheim, M. E., Church, W. R., Haley, P., and Krishnaswamy, S. (1990) *Blood* **76,** 1–16
2. Bevers, E. M., Comfurius, P., Dekkers, D. W. C., Harmsma, M., and Zwaal, R. F. A. (1998) *Biol. Chem.* **379,** 973–986
3. Esmon, C. T. (2000) *Biochim. Biophys. Acta* **1477,** 349–360
4. Esmon, C. T. (1989) *J. Biol. Chem.* **264,** 4743–4746
5. Xu, J., Esmon, N. L., and Esmon, C. T. (1999) *J. Biol. Chem.* **274,** 6704–6710
6. Regan, L. M., Mollica, J. S., Rezaie, A. R., and Esmon, C. T. (1997) *J. Biol. Chem.* **272,** 26279–26284
7. Kurosawa, S., Esmon, C. T., and Stearns-Kurosawa, D. J. (2000) *J. Immunol.* **165,** 4697–4703
8. Fukudome, K., and Esmon, C. T. (1994) *J. Biol. Chem.* **269,** 26486–26491
9. Burmeister, W. P., Gastinel, L. N., Simister, N. E., Blum, M. L., and Bjorkman, P. J. (1994) *Nature* **372,** 336–343
10. Liaw, P. C. Y., Mather, T., Oganesyan, N., Ferrell, G. L., and Esmon, C. T. (2001) *J. Biol. Chem.* **276,** 8364–8370
11. Fukudome, K., Kurosawa, S., Stearns-Kurosawa, D. J., He, X., Rezaie, A. R., and Esmon, C. T. (1996) *J. Biol. Chem.* **271,** 17491–17498
12. Otwinowski, Z., and Minor, W. (1997) *Methods Enzymol.* **276,** 307–326
13. Brunger, A. T., Adams, P. D., Clore, G. M., Delano, W. L., Gros, P., Grosse-Kunstleve, R. W., Jiang, J.-S., Kuszewski, J., Nilges, N., and Pannu, N. S. (1998) *Acta Crystallogr. Sect. D Biol. Crystallogr.* **54,** 905–921
14. Jones, T. A., Zou, J.-Y., Cowan, S. W., and Kjeldgaard, M. (1991) *Acta Crystallogr. Sect. A* **47,** 110–119
15. Taylor, F. B., Jr., Chang, A., Esmon, C. T., D'Angelo, A., Vigano-D'Angelo, S., and Blick, K. E. (1987) *J. Clin. Investig.* **79,** 918–925
16. Liaw, P. C. Y., Neuenschwander, P. F., Smirnov, M. D., and Esmon, C. T. (2000) *J. Biol. Chem.* **275,** 5447–5452
17. Cham, B. E., and Knowles, B. R. (1976) *J. Lipid Res.* **17,** 176–181
18. Zeng, Z.-H., Castano, A. R., Segelke, B. W., Stura, E. A., Peterson, P. A., and Wilson, I. A. (1997) *Science* **277,** 339–345
19. Christiansen, W. T., Jalbert, L. R., Robertson, R. M., Jhingan, A., Prorok, M., and Castellino, F. J. (1995) *Biochemistry* **34,** 10376–10382
20. Mather, T., Oganesyan, V., Hof, P., Huber, R., Foundling, S., Esmon, C., and Bode, W. (1996) *EMBO J.* **15,** 6822–6831
21. Shu, F., Kobayashi, H., Fukudome, K., Tsuneyoshi, N., Kimoto, M., and Terao, T. (2000) *FEBS Lett.* **477,** 208–212
22. Hong, S., Scherer, D. C., Singh, N., Mendiratta, S. K., Serizawa, I., Koezuka, Y., and Van Kaer, L. (1999) *Immunol. Rev.* **169,** 31–44
23. Esmon, N. L., Smirnov, M. D., and Esmon, C. T. (1997) *Thromb. Haemostasis* **78,** 79–82
24. Gu, J.-M., Ferrell, G., and Esmon, C. T. (2000) *Blood* **96,** 814a (Abstr. 3516)
25. Bacon, D. J., and Anderson, W. F. (1988) *J. Mol. Graph. Model.* **6,** 219–220
26. Kraulis, P. J. (1991) *J. Appl. Crystallogr.* **24,** 946–950
27. Honig, B., and Nicholls, A. (1995) *Science* **268,** 1144–1149